

## Extended models of the effects of point-defect dragging on dislocation motion

H. M. Simpson and A. Sosin

University of Utah, Salt Lake City, Utah 84112

(Received 3 May 1976)

The theory of defect dragging is extended to describe several distinct physical situations: the internal friction maximum due to discrete dissipative dragged defects or due to defects considered to be uniformly spread along a dislocation line, the effects of an elastic restoring force on these defects, and the effects of the variation of the dragging coefficient, particularly with temperature to yield a relaxation-type peak.

### I. INTRODUCTION

Dislocation motion due to an oscillatory stress is usually described in terms of the well-known vibrating string model of Koehler and of Granato and Lucke.<sup>1-3</sup> Basically, the dislocation is given the attributes of a string that is firmly anchored at various pinning points—dislocation nodes, jogs, and point defects. The effect of irradiation, quenching, and other experiments, which produce point defects, results in a shortening of the average free lengths of dislocation segments, in terms of the usual Koehler-Granato-Lucke interpretation. This phenomenon is called dislocation pinning. The logarithmic decrement  $\delta$  and the modulus defect  $\Delta E/E$  are sensitive indicators of the state of dislocation pinning since, in the usual Koehler-Granato-Lucke interpretation appropriate at low frequencies and low strain amplitude,

$$\delta \sim \omega \Lambda B_l l^4, \quad (1)$$

$$\Delta E/E \sim \Lambda l^2, \quad (2)$$

$$l = l_0/(1+n), \quad (3)$$

where  $\omega$  is the angular frequency of the applied stress,  $\Lambda$  is the total length of dislocation line per unit volume,  $B_l$  is the viscous damping constant of the dislocation line,  $l$  is the average length of dislocation segments between pinning points, and  $n$  is the number of pinning points added to the segments of initial length  $l_0$ . Equations (1)–(3) predict that, during irradiation, the decrement will decrease and the modulus will increase, both monotonically, as point defects are added to dislocations. We have reported recent experimental data<sup>4-8</sup> which indicate that the above interpretation of a shortening of the loop length during irradiation is not correct at frequencies below a few kHz. Evidence for this is most vividly demonstrated by the observation that, at the onset of irradiation, the decrement may *increase*, go through a maximum, and finally decrease to well below its pre-

irradiation value. Simultaneously, the modulus increases monotonically. Simpson and Sosin proposed that dislocations oscillating at fairly low frequencies (around 1 kHz) can *drag* point defects.<sup>4-9</sup> Such a dragging process is very “lossy” and can thereby give rise to a peak in the decrement as a function of irradiation time or, more fundamentally, with an increase of point defects on a dislocation line, as follows. The addition of one point defect to the line adds significantly to the energy losses. A second point defect adds an additional energy loss of its own but decreases the contribution of the first defect. At some point in the addition of further defects, the new contribution is less than the reduction from previous defects, and the energy loss maximum has been reached.

To account for the drag of point defects, Simpson and Sosin<sup>9</sup> modified the equation of motion of the vibrating string, originally presented by Koehler, by adding a viscous drag term as follows:

$$B_l \frac{\partial y(x, t)}{\partial t} + \sum_{i=1}^n B_d \delta(x - x_i) \frac{\partial y(x, t)}{\partial t} - C \frac{\partial^2 y(x, t)}{\partial x^2} = b \sigma_0 e^{-i \omega t}, \quad (4)$$

where  $y$  is the displacement of the dislocation from its equilibrium position at a position  $x$  at time  $t$ ;  $B_l$  is the viscous drag associated with the line (but not necessarily the usual line damping term—see the following discussion);  $B_d$  is the viscous drag coefficient of a point defect located at  $x = x_i$ ;  $C$  is the line tension;  $b$  is the magnitude of the Burgers vector; and  $\sigma_0$  is the magnitude of the applied stress of angular frequency  $\omega$ . The boundary conditions on Eq. (4) are

$$y(0, t) = y(l, t) = 0. \quad (5)$$

At this point it should be stressed that in our formulation the loop length  $l$  remains fixed and the addition of point defects is accounted for in the viscous drag term,

$$\sum_{i=1}^n B_d \delta(x-x_i) \frac{\partial y(x,t)}{\partial t}.$$

The steady-state solution for the displacement, as given by Simpson and Sosin,<sup>9</sup> for one point defect

$$G(x, x_i) = \left( \alpha \sinh \frac{l}{\alpha} \right)^{-1} \left[ \sinh \left( \frac{l-x_i}{\alpha} \right) \sinh \left( \frac{x}{\alpha} \right) \Theta(x_i - x) + \sinh \left( \frac{x_i}{\alpha} \right) \sinh \left( \frac{l-x}{\alpha} \right) \Theta(x - x_i) \right], \quad (6b)$$

$$\Theta(a) = \begin{cases} 0, & a < 0 \\ 1, & a > 0 \end{cases}, \quad (6c)$$

$$y_0(x) = \frac{i \sigma_0 b}{\omega B_l \sinh(l/\alpha)} \times \left[ \sinh \left( \frac{l}{\alpha} \right) - \sinh \left( \frac{x}{\alpha} \right) - \sinh \left( \frac{l-x}{\alpha} \right) \right], \quad (6d)$$

$$\alpha^2 = iC/\omega B_l. \quad (6e)$$

To evaluate  $y(x_i)$ , simply set  $x=x_i$  in Eq. (6a).

In the original treatment of Simpson and Sosin, emphasis was placed on showing that the peaking effect in the decrement could be accounted for in terms of the drag model. Now that this has been firmly established experimentally, an extended analysis of the consequences of defect dragging is in order. This is a primary purpose of this paper.

Recently, Mizubayashi and Okuda<sup>10</sup> presented a series of plots for the modulus defect and decrement which were generated from Eqs. (6a)–(6e) above. In a number of cases they obtained theoretical results which were physically unattainable, as noted by them. This was due in part to their choice of plotting parameters. It is also our purpose to present here the theory in a form that emphasizes those parameters which can be affected most directly by experiment; i.e., emphasis will be placed on the physical aspects of the theory. To achieve these purposes, we will analyze Eqs. (4)–(6) under different interpretations and transformations. It is important that the physical interpretation of the parameters be clearly stated and appreciated to obtain an understanding of the phenomenological conclusions.

## II. CALCULATIONS

### A. Average displacement of the dislocation

The appropriate theoretical quantities of interest in every case are the real and imaginary parts of the average displacement  $\bar{y}$  of the dislocations, since the logarithmic decrement is proportional to  $\text{Im}(\bar{y})$  and the modulus defect is proportional to  $\text{Re}(\bar{y})$ . To simplify the analysis, one point

located at  $x=x_i$ , is

$$y(x) = y_0(x) - (B_d/B_l)y(x_i)G(x, x_i), \quad (6a)$$

with

defect is assumed to be located at the center of the line. In our plots we present the real and imaginary parts of the normalized average displacement  $\bar{y}_n$  which is

$$\begin{aligned} \bar{y}_n &\equiv [C(\sigma_0 b l^2)^{-1}] \bar{y} \\ &= (Z^2 \sinh Z)^{-1} \{ \sinh Z - 2Z^{-1}(\cosh Z - 1) \\ &\quad - Z^{-1}[i \mu_d^{-1} Z \sinh Z + \sinh^2(\frac{1}{2}Z)]^{-1} \\ &\quad \times [\sinh Z - 2 \sinh(\frac{1}{2}Z)]^2 \}, \quad (7a) \end{aligned}$$

with

$$Z \equiv (\frac{1}{2} \omega B_l l^2 C^{-1})^{1/2} (1-i) \equiv \mu_l (1-i), \quad (7b)$$

$$\mu_d = \omega B_d l C^{-1}. \quad (7c)$$

In some cases, as noted by Mizubayashi and Okuda,<sup>10</sup> it might be interesting to consider the effects of a linear restoring force of magnitude  $K\delta(x-x_i)y(x,t)$  acting on a point defect at  $x=x_i$ , where  $K$  is the force constant. When this term is added to Eq. (4), the only change in the resulting expression for  $\bar{y}_n$  is to let

$$\mu_d \rightarrow \mu_d + i \mu_\kappa, \quad (8a)$$

with

$$\mu_\kappa \equiv K l C^{-1}. \quad (8b)$$

In this manner one can examine the effects of both a linear restoring force and a viscous drag force either simultaneously or separately.

For the work reported here, Eq. (7) was evaluated on a Univac 1108 computer which automatically separated ( $\bar{y}_n$ ) into its real and imaginary parts and generated the appropriate graphs of these quantities. [For details on the mathematical procedure to go from  $\bar{y}_n$  to (normalized) decrement and (normalized) modulus, see Ref. 9.]

### B. Case I: Viscous drag in the smeared-out limit

The normalized decrement,  $\text{Im}(\bar{y}_n)$ , is plotted as a function of  $\mu_l$  for various values of the drag parameter  $\mu_d$  in Fig. 1. Of particular interest here is the case of  $\mu_d=0$ . For this case, the point defects are "smeared" out along the dislocation line and  $B_l$  is identified as the drag coefficient of this ensemble of smeared-out defects. Then, on

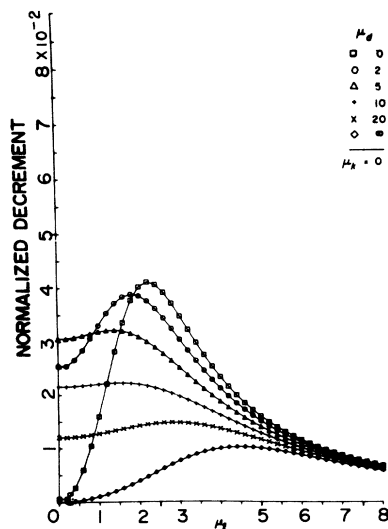


FIG. 1. Normalized decrement is plotted as a function of the dislocation line damping parameter  $\mu_l$ . The influence of the addition of discrete point defects to the line is followed by observing the decrement at a fixed value of the abscissa as  $\mu_d$  increases. However, the plot may be read differently also, in the "smeared-out" limit, using the  $\mu_d = 0$  curve. In this case, the discrete points are imagined to be spread uniformly along the dislocation line, leading to an increase in  $\mu_l$ . Accordingly, the decrement is followed along the  $\mu_d = 0$  curve for increasing  $\mu_l$ . Note that the  $\mu_d = \infty$  curve can be translated into the  $\mu_d = 0$  curve by multiplying the abscissa values by  $\frac{1}{2}$  and the ordinate values by 4.

the addition of point defects,  $B_l$  changes according to

$$B_l = B_0 + nB', \quad (9)$$

where  $B_0$  is the viscous drag constant for defects which produce the background (e.g., pre-irradiation) damping and  $nB'$  is the increment due to the added defects. If  $\omega$ ,  $l$ ,  $c$ , and  $B_0$  are of appropriate magnitude (i.e., so that  $\mu_l < 2.2$ ) then the decrement will increase and go through a maximum on the addition of draggers. This has been observed experimentally a number of times.<sup>4-8, 11-13</sup> Depending on the magnitude of the initial value of  $\mu_l$ , the decrement can either increase or decrease. However, as seen from Fig. 2, the modulus defect always decreases for an increase in  $\mu_l$  for the special case of  $\mu_d = 0$ .

At the other limit, we have the case of  $\mu_d = \infty$ . In fact, these two extreme cases are basically the same. When  $\mu_d = \infty$ , we have two lines, each of length  $\frac{1}{2}l$ , and the same previous comments made about the results for  $\mu_d = 0$  apply here. The only change is in the magnitude of the modulus defect and the damping.

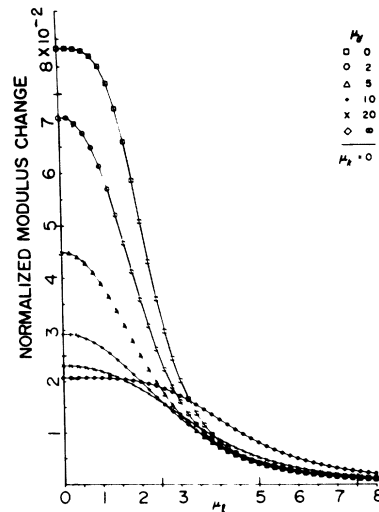


FIG. 2. Companion plot to Fig. 1 for the normalized defect, instead of the decrement.

### C. Case II: Viscous drag with discrete draggers

The general case of a nonzero finite  $\mu_d$  shows that, if  $\mu_l$  is low, the addition of a dragger always increases the damping and decreases the modulus defect. For  $\mu_l \geq 1.5$  the modulus defect *increases* in some cases on the addition of a dragger, an effect we failed to observe originally but was noted by Okuda and Mizubayashi. This is particularly noticeable if the drag coefficient is infinite; i.e.,

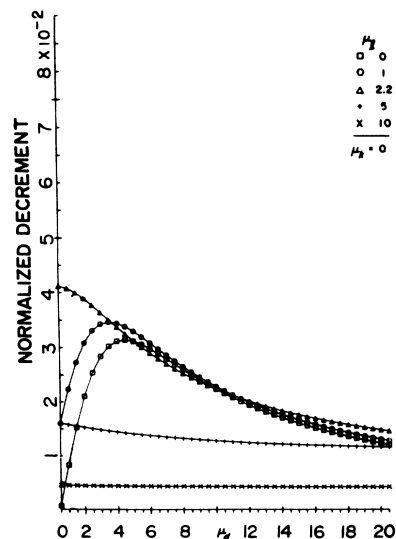


FIG. 3. Normalized decrement is plotted as a function of the defect drag parameter  $\mu_d$  for several values of dislocation line damping, given by  $\mu_l$ . For  $\mu_l < 2.2$  a peaking effect is produced; for  $\mu_l > 2.2$ , the decrement decreases monotonically as  $\mu_d$  increases. Note that  $\mu_d$  can vary due to several causes, as discussed in the text.

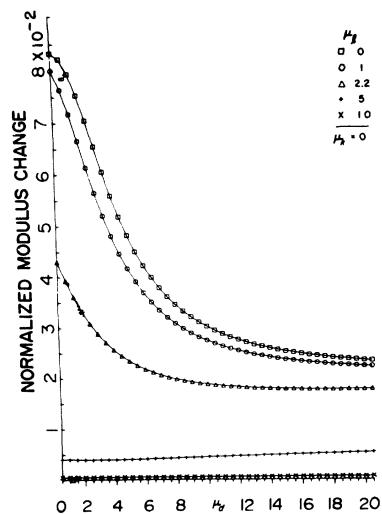


FIG. 4. Companion plot to Fig. 3 for the normalized modulus change, instead of the decrement.

a firm pinner. Experimental results of this nature have been reported by Okuda and Mizubayashi.<sup>14</sup>

In Figs. 3 and 4 we have plotted the normalized decrement and modulus defect, respectively, as a function of  $\mu_d$  for various values of the parameter  $\mu_l$ , giving rise to a relaxation-type damping peak; see further below. For a certain range of  $\mu_l$ , the damping would go through a peak as  $\mu_d(B_d)$  varied.

#### D. Linear restoring force and viscous drag

The presence of a linear restoring force (LRS) on a dragged point defect will always cause the decrement to be lower than it would otherwise. This is made evident in a comparison of the decrement curves of Figs. 5(a), 5(b), and 5(c), with those of Fig. 1. An examination of Fig. 5(a) shows that, for a fixed  $\mu_l$ , the decrement decreases as  $\mu_k$  increases. However, if a viscous drag is also present along with the LRS, the decrement can either increase or decrease upon the addition of a dragger to a dislocation line, depending on the magnitude of  $\mu_d$ ,  $\mu_l$ , and  $\mu_k$ .

For low values of  $\mu_l$ , the modulus defect is reduced when the dragger experiences a LRS. Physically, this is to be expected since the LRS simply retards the motion of the point defect and thereby also hinders the displacement of the dislocation line. Evidence for this effect is given in Figs. 6(a), 6(b), and 6(c). At high values of  $\mu_l$  one observes an anomalous increase in the modulus defect as the LRS becomes larger. This is particularly noticeable when the LRS becomes infinite; i.e., the point defect is a firm pinner.

Earlier in this article, we presented an account

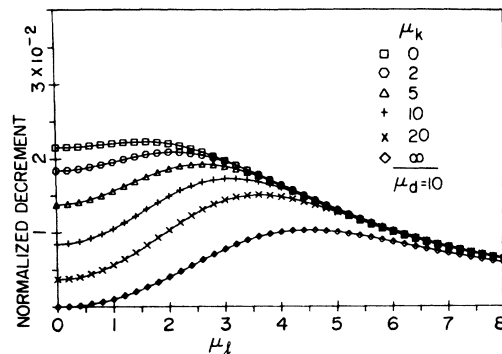
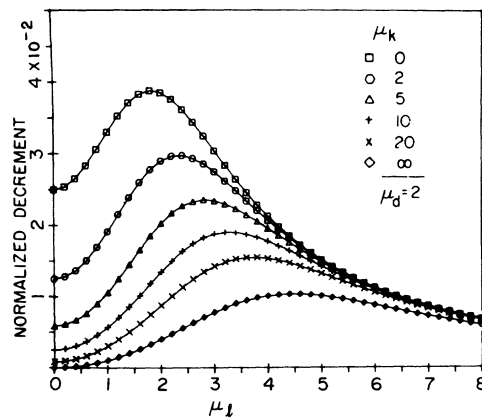
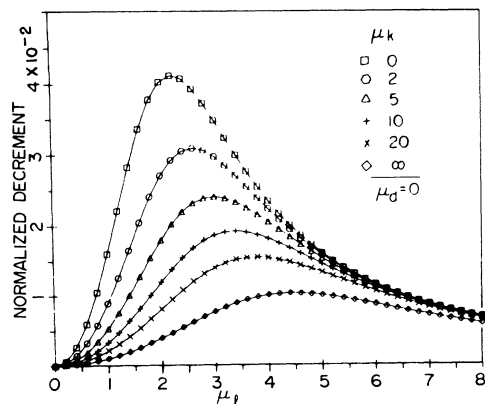


FIG. 5. Influence of a linear restoring force, given by the parameter  $\mu_k$ , working on defects attached to a dislocation on the normalized decrement.

of the physics which leads to an internal friction maximum. The increase in the modulus defect is more subtle. In the limit of high  $\mu_l$ , the motion of the dislocation line is  $90^\circ$  out of phase with the driving force, giving rise to zero modulus defect since the modulus defect arises from in-phase motion. The anomalous modulus defect phenomenon can be traced to enhanced in-phase motion brought on by the addition of point defects on the dislocation line. The effect is fundamentally one of phase consideration and, accordingly, appears

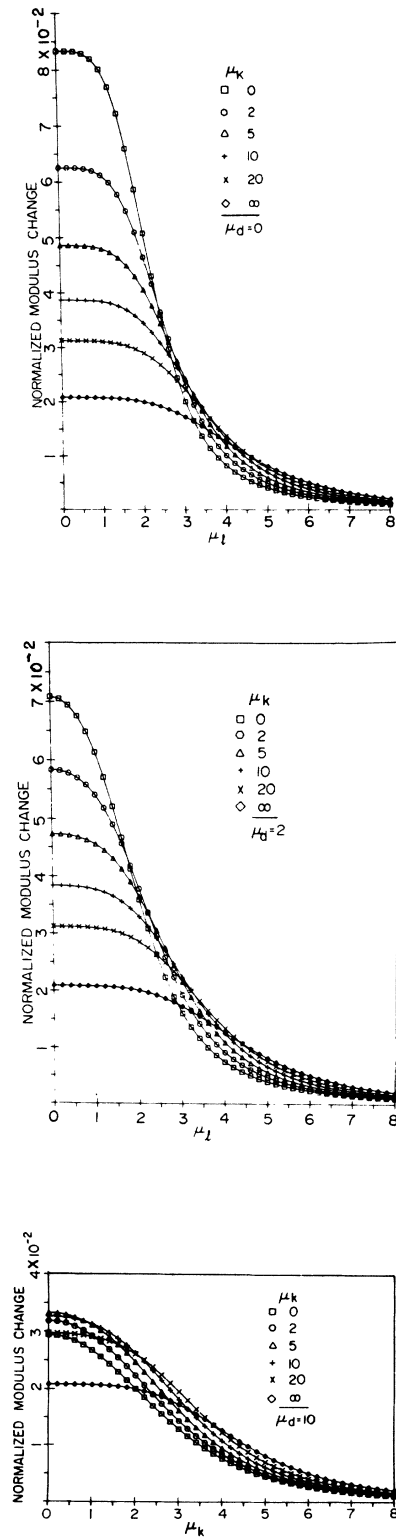


FIG. 6. Companion plot to Fig. 5 for the normalized modulus defect, instead of the decrement.

anomalous; one generally ascribes a modulus defect to enhanced strain accompanying dislocation motion.

E. Case IV: Temperature-dependent viscous drag

The mobility of a point defect on a dislocation might be very temperature dependent. For example, if the defect (point defect, jog, or kink) undergoes stress-assisted diffusion when it is attached to an oscillating dislocation, the drag coefficient should be governed by a Boltzmann factor. At high temperatures the mobility of the defect would be so large that it would offer no viscous drag; however, at low temperature the defect would be essentially frozen in place, thereby merely shortening the average length of dislocation segments. Thus the damping would be low at low temperatures, increase as the temperature is increased, and finally approach a limiting value at high temperatures. The high-temperature damping is due to line damping. Such behavior of the damping as a function of temperature would give a relaxation-type internal friction peak.

To investigate the nature of the relaxation-type peak due to a temperature-dependent drag coefficient we arbitrarily take  $\mu_d = 4 \times 10^{-10} \exp(0.12/kT)$  and  $\mu_k = 0$ . The appropriate decrement and modulus plots are given in Figs. 7 and 8, respectively. As expected, the damping goes through a peak at some characteristic temperature. The damping is high on the high-temperature side of the peak and considerably reduced on the low-temperature side. This behavior is typically observed in Bordoni-type relaxation peaks.

The effects of irradiation on the relaxation peak

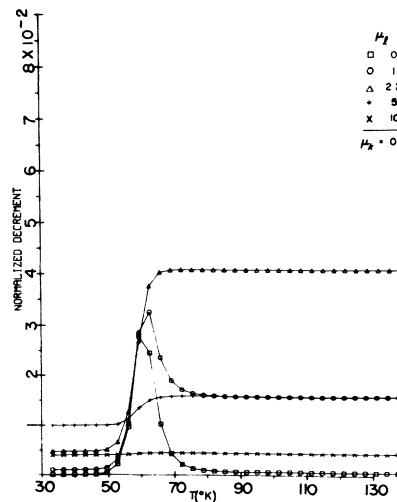


FIG. 7. Production of a relaxation-type peak in the decrement, due to an Arrhenius temperature dependence of the defect drag parameter  $\mu_d$ .

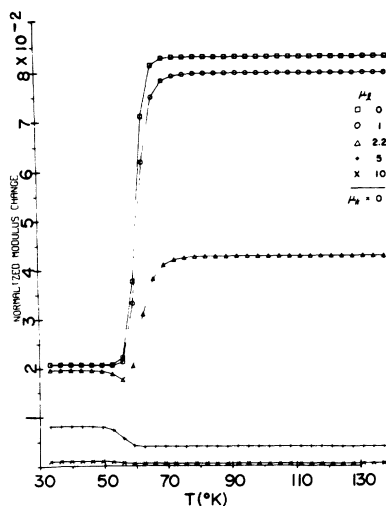


FIG. 8. Companion plot to Fig. 7 for the normalized modulus defect.

can be understood by assuming that  $B_i$  increases as point defects are added to the dislocation. This, of course, increases  $\mu_i$  via Eq. (7b) and (9). For this model to have merit, it is essential that an

intrinsic defect be present on the dislocation prior to irradiation and that it be of a different type than that introduced by the irradiation. Feltham<sup>15</sup> has suggested that the *drag* of jogs, intrinsic to dislocations, could give rise to the Bordoni peak.

### III. SUMMARY

In this paper we have presented a series of graphs of the logarithmic decrement and modulus defect as functions of various drag parameters. The analytical solutions were based on extensions of the Simpson-Sosin model of dislocation drag of point defects, to include viscous drag of attached defects and a linear restoring force on the point defect. The model is sufficiently versatile that it can easily account for (i) the peaking effect observed in the decrement during irradiation, and (ii) relaxation-type internal friction peaks such as the Bordoni peak.

### ACKNOWLEDGMENT

We wish to thank D. Lee for the programming reported here. This work was supported by the Division of Materials Research of the National Science Foundation.

- <sup>1</sup>J. S. Koehler, in *Imperfections in Nearly Perfect Crystals*, edited by W. Shockley (Wiley, New York, 1952), p. 197.
- <sup>2</sup>A. V. Granato and K. Lucke, *J. Appl. Phys.* **27**, 583 (1956).
- <sup>3</sup>A. V. Granato and K. Lucke, *J. Appl. Phys.* **27**, 789 (1956).
- <sup>4</sup>H. M. Simpson, A. Sosin, G. R. Edwards, and S. L. Seiffert, *Phys. Rev. Lett.* **26**, 897 (1971).
- <sup>5</sup>H. M. Simpson, A. Sosin, and S. L. Seiffert, *J. Appl. Phys.* **42**, 3977 (1971).
- <sup>6</sup>H. M. Simpson, A. Sosin, and D. F. Johnson, *Phys. Rev. B* **5**, 1393 (1972).
- <sup>7</sup>S. L. Seiffert, H. M. Simpson, and A. Sosin, *J. Appl. Phys.* **44**, 3404 (1973).

- <sup>8</sup>H. M. Simpson and S. J. Kerkhoff, *Phys. Rev. Lett.* **33**, 155 (1974).
- <sup>9</sup>H. M. Simpson and A. Sosin, *Phys. Rev. B* **5**, 1382 (1972).
- <sup>10</sup>H. Mizubayashi and S. Okuda, *Radiat. Eff.* **21**, 185 (1974).
- <sup>11</sup>R. L. Nielsen, Ph.D. dissertation (University of Pittsburgh, 1968) (unpublished).
- <sup>12</sup>J. L. Routbort and H. S. Sack, *J. Appl. Phys.* **37**, 4803 (1966).
- <sup>13</sup>J. Louzier, C. Minier, and S. L. Seiffert, *Philos. Mag.* **31**, 893 (1975).
- <sup>14</sup>S. Okuda and H. Mizubayashi, *Radiat. Eff.* **25**, 57 (1975).
- <sup>15</sup>P. Feltham, *Philos. Mag.* **13**, 913 (1966).